MKE Scheme for Planning and Control of Dual-arm Robotic System Aided with Recurrent Neural Networks

Jialiang Fan*†‡§, Mei Liu†‡§, Shuai Li*, *Senior Fellow, IEEE*
*School of Information Science and Engineering, Lanzhou University, Lanzhou 730000, China.
†Chongqing Institute of Green and Intelligent Technology, Chinese Academy of Sciences, Chongqing 400714, China
‡University of Chinese Academy of Sciences, Beijing 100049, China
§Key Laboratory of Medical Imaging, Lanzhou University Second Hospital, Lanzhou 730000, China
Email: fjl2401@163.com, liumeisysu@qq.com, lishuai@lzu.edu.cn

2021 International Joint Conference on Neural Networks (IJCNN) | 978-1-6654-3900-8/21/$31.00 ©2021 IEEE | DOI: 10.1109/IJCNN52387.2021.9533914

***Abstract*—Dual-arm robotic systems have great advantages over the single-arm robotic system, for the arms can either run independently or cooperate to finish the task. In this paper, minimum kinetic energy (MKE) is concerned as a performance index for the planning and control of a dual-arm robotic system. First, two subschemes are formulated on the left arm and right arm of the robot, which are constructed on velocity level with consideration of manipulators' physical constraints. Then, the two subschemes are unified into one scheme, which is finally transformed into a quadratic program (QP) problem. For solving the formulated QP problem, a recurrent neural network (RNN) is devised based on the Lagrange multiplier method. At last, the simulations and simulative experiments on a dual-arm redundant robotic system named Baxter are carried out. The simulation results reveal that the devised RNN model has a good performance for solving the presented MKE scheme applying to the dual-arm robotic system.**

***Index Terms*—minimum kinetic energy (MKE), dual-arm robotic system, quadratic program (QP), Lagrange multiplier method, recurrent neural network (RNN).**

I. Introduction

With the development of the manufacturing industry field, the automation field, the computer science field [1]–[3], etc., manipulators are playing an increasingly critical role in human life and have been applied in industrial, military, and medical areas. Besides, manipulators can liberate humans from doing dirty, dangerous, and dull jobs or executing the high accuracy required tasks that humans are not up to, such as welding, casting, and so on [4], [5]. The redundant manipulator is a special case of manipulators, which has more degrees of freedom (DOFs) beyond the task required. The extra DOFs give the manipulator more choices for executing a given task, thereby satisfying the secondary task such as obstacle avoidance, minimization of energy consumption during the task execution. There always exist infinite solutions for taking the motion control of the redundant manipulator from the joint level due to the manipulator's redundancy. Sometimes the optimal solution can be found with the consideration of equality constraints or inequality constraints. However, the mapping from joint space to Cartesian space is usually nonlinear, and the problem is difficult to be solved directly with the desired accuracy. Thus, a better way is investigating the problem on the velocity or acceleration level, and the problem is transformed into a linear problem, because the mapping from joint space to Cartesian space is presented as an affine system [6].

In addition, the performance index is playing a significant role in quadratic program (QP) based manipulator control scheme, because different performance indexes reflect the characteristics of the manipulator in different scenarios, which determine the application potential of redundant manipulators in industry fields [7]. Therefore, setting up an efficient performance index for redundant manipulator planning and control is an important issue. Minimum kinetic energy (MKE) is a popular performance index and has been widely used by researchers for high-accuracy control and planning of the manipulator [8]. Compared with minimum velocity norm (MVN), the MKE performance index is more rational in terms of kinetic-energy consumption, because it takes the minimizing of the weighted sum of joint velocities as the objective function and can be considered as the local counterpart of the global kinetic energy minimization scheme [9], [10]. In this sense, the MKE performance index is better than the MVN performance index in the control and planning of manipulators.

Intelligent computing technology figures out many challenging problems with the increase of calculation power [11]–[14]. For example, Luo *et. al* exploit the gradient descent methods on recommender systems and achieve great progress [15]–[17]. Besides, the research results are also utilized in industrial

This work was supported in part by the Gansu Province Key Laboratory of Medical Imaging Fund Project under Grant 18JR2RA028, in part by the research project of Huawei Mindspore Academic Award Fund of Chinese Association of Artificial Intelligence under Grant CAAIXSJLJJ-2020-012A, in part by the Natural Science Foundation of Gansu Province, China, under Grant 20JR10RA639, in part by the Natural Science Foundation of Chongqing (China) under Grant cstc2020jcyj-zdxmX0028, in part by the Research and Development Foundation of Nanchong (China) under Grant 20YFZJ0018, in part by CAS "Light of West China" Program. *(Jialiang Fan and Mei Liu are co-first authors.)*

fields [18]–[22]. As a powerful tool in intelligent computing fields, the neural network has attracted bunches of researchers' attention for its superior ability in dealing with massive and complicated calculations [23]–[25]. Many developers and researchers devote themselves to improve the usage of neural networks. For example, a noise-suppressing recurrent neural network model is constructed in [26], which has an extensive prospect in the fields of robotics and acoustics. In [27], a reformative noise-immune neural network is presented, with excellent robustness and efficiency on image target detection. Zhang *et. al* achieve great progress by applying the neural networks on distributed robotic systems control [28], [29]. Besides, a powerful deep learning framework named MindSpore is becoming increasingly popular, for it greatly improves the efficiency of using intelligent computing technology [30]. The neural network has an excellent data processing performance compared to conventional computing methods, especially on real-time task [31], [32]. Solving the QP based scheme of the redundant manipulator planning and control via the neural network is a promising research direction. In [33], a dual neural network is devised to address the redundancy resolution problem of the manipulator, which does not require prior knowledge of the manipulator. As a special case of neural networks, the recurrent neural network (RNN) has been widely exploited and investigated by researchers. For example, Xu *et. al* present a novel motion-force control problem with consideration of joint constraints, and the problem is finally transformed to a QP problem and solved by an elaborately devised neural network [34]. Li *et. al* present a novel RNN for solving redundancy resolution of manipulators in the presence of polynomial noises [35].

Investigations on the dual-arm robotic system have become increasingly prevalent in recent years for their significant advantages over single-arm robots. The dual-arm means the system has two independent manipulators that can either run the task independently or cooperate to finish more complex tasks [36]. In [37], a dual-arm robotic system is built in a coordinated manner, and the affiliated manipulator will follow the main manipulator when the main manipulator executes the task. Besides, the constraints between the robot and the objective are maintained.

This paper considers the MKE as the performance index of planning and control of the redundant manipulator. More specifically, the MKE scheme on the dual-arm, i.e., the left arm and the right arm, is formulated respectively. Afterward, the two subschemes are unified into a single scheme, which can be considered as a QP problem. For solving the QP problem, an RNN aided with the Lagrange multiplier method is devised. Finally, the simulations and simulative experiments are carried out on the Baxter robot with two identical 7-DOF redundant manipulators. The simulation results reveal the correctness and accuracy of the solution for the unified scheme and depict the states of two manipulators at different time instants when performing the task. Before ending this part, the contributions of this paper can be summarized as below:

- This paper focuses on investigating the MKE performance index of redundant manipulator control on joint velocity level, and the definition of the inertia matrix in the MKE scheme is first and clearly given and explained.
- For the first time, the MKE scheme is investigated and applied on the dual-arm robotic system, and the schemes on the left arm and right arm are unified into one scheme, thereby extending the research fields to the dual-arm robotic system.
- For solving the formulated problem, an RNN aided with the Lagrange multiplier method is devised, and physical constraints are taken into consideration for protecting the manipulator.
- The simulation results on Baxter robot for tracking predefined trajectory verify the correctness and accuracy of the MKE scheme, and the simulative results on CoppeliaSim robotic visualization system vividly validate the scheme in a further step.

II. Preliminaries, scheme construction and solutions

In the section, first, we revisit the forward kinematic problem and the definition of MKE performance index. Then, the MKE scheme is applied on the left arm and right arm of the dual-arm robotic system considering physical constraints. Subsequently, the two schemes are unified into one scheme, which is a QP problem. Finally, for solving the QP problem, an RNN based on the Lagrange multiplier method is devised, and the corresponding analytical solution is presented as well.

A. Revisiting forward kinematic problem

The forward kinematic problem is concerned with the relationship between the position of each joint and the position and orientation of the end-effector. Stated more formally, the forward kinematic problem is to calculate the position and orientation of the end-effector when the joint values of the manipulator are given, which can be presented as the following equation:

$$f(\boldsymbol{\theta}) = \mathbf{p}, \tag{1}$$

where $\boldsymbol{\theta} \in \mathbb{R}^m$ represents the joint angle in joint space, and $\mathbf{p} \in \mathbb{R}^n$ $(m > n)$ represents the state of manipulator in Cartesian space. The mapping function f from joint space to Cartesian space is nonlinear, and the solution is usually difficult to be found directly. To solve it numerically, we can take the derivative to both sides of equation (1), and we get the following equation:

$$J(\boldsymbol{\theta})\dot{\boldsymbol{\theta}} = \dot{\mathbf{p}}, \tag{2}$$

where $J(\boldsymbol{\theta}) = \partial f(\boldsymbol{\theta})/\partial \boldsymbol{\theta} \in \mathbb{R}^{n\times m}$ is a time-varying Jacobian matrix, which establishes a linear transformation between the joint space and Cartesian space, thereby making the problem more easily to be dealt with; $\dot{\boldsymbol{\theta}}$ and $\dot{\mathbf{p}}$ represent the real-time velocity in joint space and Cartesian space, respectively.

B. Revisiting MKE performance index

MKE of the planning and control of the manipulator is to minimize the weighted sum of squares of joint velocities, which is a popular performance index used by the great majority of investigators [9], [38], [39]. In this paper, the MKE problem is investigated from the perspective of joint velocity level with consideration of physical constraints. For laying a foundation to further research, the MKE problem is presented as

$$\min \quad \dot{\boldsymbol{\theta}}^{\mathrm{T}} V \dot{\boldsymbol{\theta}}/2 \tag{3a}$$

$$\text{s.t.} \quad \dot{\mathbf{p}}_{\mathrm{d}} = J\dot{\boldsymbol{\theta}} \tag{3b}$$

$$\dot{\boldsymbol{\theta}} \in \Omega, \tag{3c}$$

where $V \in \mathbb{R}^{m\times m}$ is a positive-definite and symmetric inertia matrix; $\mathbf{p}_{\mathrm{d}}$ is the desired end-effector trajectory of the manipulator; Ω denotes the set of feasible regions of joint velocity, which is designed as $\Omega = \{\dot{\boldsymbol{\theta}} \in \mathbb{R}^m, \boldsymbol{\beta}^- \leq \dot{\boldsymbol{\theta}} \leq \boldsymbol{\beta}^+\}$ in existing works [40], [41], with $\boldsymbol{\beta}^-$ and $\boldsymbol{\beta}^+$ representing the lower bound and upper bound of velocities in joint space, respectively. The objective function (3a) is aiming to minimize the kinetic energy consumption of the manipulator, which can be considered as making the joint with the greater mass move as little as possible; the equality constraint of (3b) guarantees that the manipulator will move along the predefined trajectory [42]; the inequality constraint (3c) guarantees that the joint velocities of manipulator during the task are within the range of physical constraints.

Revisiting that minimizing kinetic energy consumption of the manipulator can be considered as minimizing the weighted sum of squares of velocities on each joint, the weighted part expressed in equation (3) is the inertia matrix $V \in \mathbb{R}^{m\times m}$. In this paper, the inertia matrix V is defined as a diagonal matrix, and the first element on the diagonal represents the weight of energy consumption to move the first joint, which is defined as the sum of this joint and rest joints' mass. The mass of each joint can be found from Table I [43].

Remark 1: We discuss the MKE performance index and display the corresponding objective function, in which the physical constraints are considered, and the solution is investigated on the joint velocity level. Then, we give a detailed and precise description of the definition of the inertia matrix V used in this paper, which makes the MKE scheme more comprehensible from a realistic point of view.

TABLE I
D-H PARAMETERS OF THE BAXTER ROBOT.

link	θ	d (m)	a (m)	α (rad)	m (kg)
1	θ_1	0.2703	0.069	$-\pi/2$	5.70044
2	θ_2	0	0	$\pi/2$	3.22698
3	θ_3	0.3644	0.069	$-\pi/2$	4.31272
4	θ_4	0	0	$\pi/2$	2.07206
5	θ_5	0.3743	0.01	$-\pi/2$	2.24665
6	θ_6	0	0	$\pi/2$	1.60979
7	θ_7	0.2295	0	0	0.54218

C. The scheme applying on a dual-arm robotic system

In this subsection, we apply the MKE scheme presented in the last subsection on the dual-arm robotic system, and the schemes on the left manipulator and right manipulator are presented. Besides, the two subschemes are unified as one scheme, which is finally transformed into a QP problem.

For the dual-arm robotic system, two manipulators can execute the given task independently, which means that if the two manipulators are given the task with the same period, the task completion states of the two manipulators at any moment are consistent and the two manipulators will finish the task simultaneously. Given this situation, the planning and control problems of the left manipulator and right manipulator can be unified into one problem. The MKE scheme applied on the left manipulator is presented as

$$\min \quad \dot{\boldsymbol{\theta}}_{\mathrm{l}}^{\mathrm{T}} V_{\mathrm{l}} \dot{\boldsymbol{\theta}}_{\mathrm{l}}/2 \tag{4a}$$

$$\text{s.t.} \quad \dot{\mathbf{p}}_{\mathrm{ld}} = J_{\mathrm{l}}\dot{\boldsymbol{\theta}}_{\mathrm{l}} \tag{4b}$$

$$\dot{\boldsymbol{\theta}}_{\mathrm{l}} \in \Omega_{\mathrm{l}}, \tag{4c}$$

of which $\dot{\boldsymbol{\theta}}_{\mathrm{l}}$ represents the joint velocity of left arm; $\boldsymbol{\theta}_{\mathrm{l}}$ denotes the joint angular value of left arm; $\dot{\mathbf{p}}_{\mathrm{ld}}$ denotes the desired end-effector velocity; the definitions of J_{l}, Ω_{l} are the same as those discussed in equation (3). Likewise, the MKE scheme on right arm of dual-arm robotic system is similar to the left arm:

$$\min \quad \dot{\boldsymbol{\theta}}_{\mathrm{r}}^{\mathrm{T}} V_{\mathrm{r}} \dot{\boldsymbol{\theta}}_{\mathrm{r}}/2 \tag{5a}$$

$$\text{s.t.} \quad \dot{\mathbf{p}}_{\mathrm{rd}} = J_{\mathrm{r}}\dot{\boldsymbol{\theta}}_{\mathrm{r}} \tag{5b}$$

$$\dot{\boldsymbol{\theta}}_{\mathrm{r}} \in \Omega_{\mathrm{r}}, \tag{5c}$$

Note that the definitions of $\dot{\boldsymbol{\theta}}_{\mathrm{r}}$, V_{r}, $\dot{\mathbf{p}}_{\mathrm{rd}}$, J_{r} and Ω_{r} on right arm MKE scheme are similar to those on the left arm. As we previously discussed, the two manipulators of the dual-arm robotic system will execute the given task simultaneously. Therefore, the two schemes can be unified into one as below:

$$\min \quad \dot{\boldsymbol{\tau}}^{\mathrm{T}} H \dot{\boldsymbol{\tau}}/2 \tag{6a}$$

$$\text{s.t.} \quad \boldsymbol{\omega}_{\mathrm{d}} = W\dot{\boldsymbol{\tau}} \tag{6b}$$

$$\dot{\boldsymbol{\tau}} \in \Omega, \tag{6c}$$

where

$$\boldsymbol{\tau} = \begin{bmatrix} \boldsymbol{\theta}_{\mathrm{l}} \\ \boldsymbol{\theta}_{\mathrm{r}} \end{bmatrix} \in \mathbb{R}^{2m},\ H = \begin{bmatrix} V_{\mathrm{l}} & 0 \\ 0 & V_{\mathrm{r}} \end{bmatrix} \in \mathbb{R}^{2m\times 2m},$$

$$\boldsymbol{\omega}_{\mathrm{d}} = \begin{bmatrix} \dot{\mathbf{p}}_{\mathrm{ld}} \\ \dot{\mathbf{p}}_{\mathrm{rd}} \end{bmatrix} \in \mathbb{R}^{2n},\ W = \begin{bmatrix} J_{\mathrm{l}} & 0 \\ 0 & J_{\mathrm{r}} \end{bmatrix} \in \mathbb{R}^{2n\times 2m}.$$

Note that the dimension of the unified Jacobian matrix W is $2n \times 2m$. In this paper, we consider the position of the manipulator's end-effector and ignore the orientation of the end-effector, thus, the dimension of desired end-effector velocity $\dot{\mathbf{p}}_d$ for a single arm is 3×1, and the dimension of corresponding Jacobian matrix is $3\times m$. Hereto, the unification of MKE scheme of dual-arm robotic system is finished.

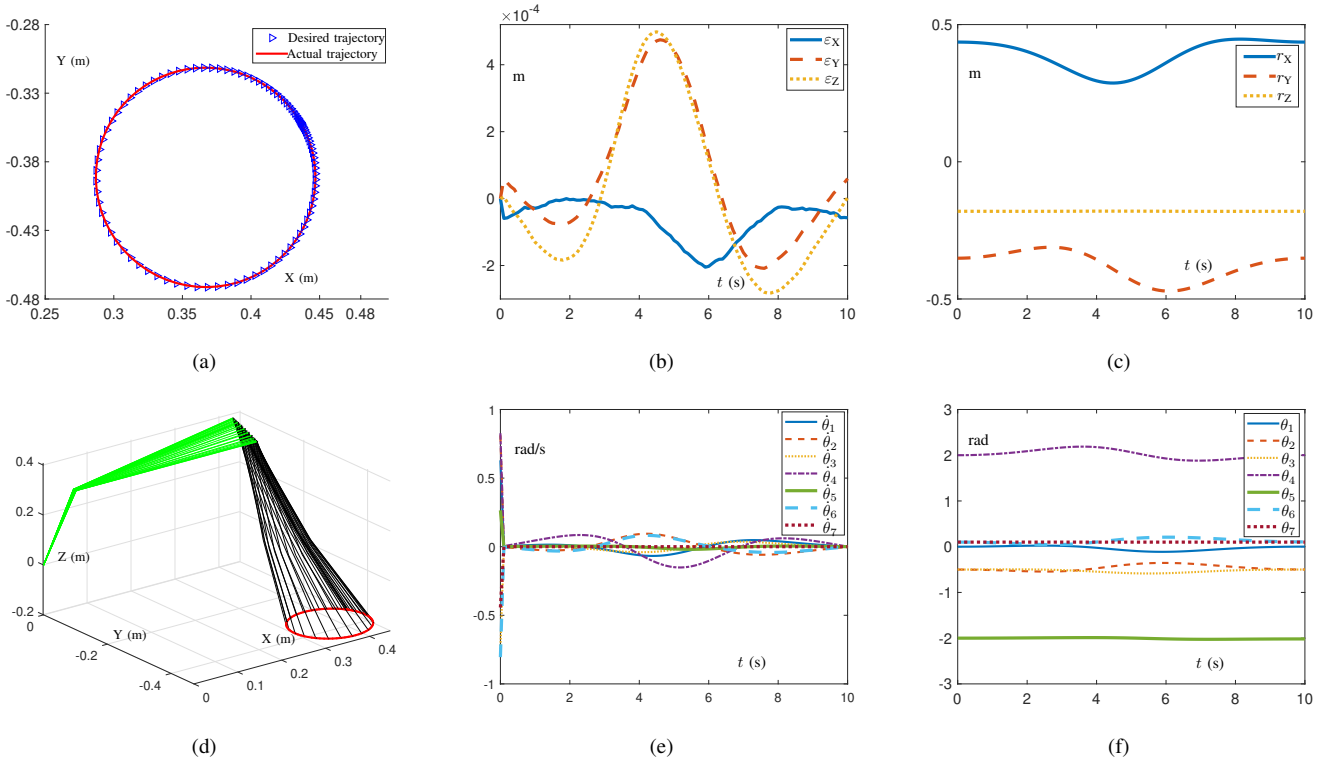

Fig. 1. The simulation results of the left manipulator on the Baxter robot. (a) Real trajectory and desired trajectory of the left manipulator. (b) Time history of the end-effector errors on the left manipulator during the task. (c) Time history of the end-effector positions on the left manipulator during the task. (d) The motion trajectories of the left manipulator. (e) Time history of the joint velocities of the left manipulator. (f) Time history of the joint angles of the left manipulator.

D. The corresponding RNN

In this section, in order to find a solution to the unified QP problem presented in the last subsection, a Lagrange function is devised. Then, for finding the optimal solution of the objective function, the partial derivative is taken with the aid of the Lagrange multiplier, and the problem is transformed to a nonlinear equation, which is hard to solve directly. According to the work in [44], [45], an RNN is devised aided with the Lagrange multiplier method. Finally, the resolutions are conducted for the RNN.

Firstly, define a Lagrange function as below:

$$L = \dot{\boldsymbol{\tau}}^{\mathrm{T}} H \dot{\boldsymbol{\tau}}/2 + \boldsymbol{\lambda}(\boldsymbol{\omega}_{\mathrm{d}} - W\dot{\boldsymbol{\tau}}), \tag{7}$$

where $\boldsymbol{\lambda} > 0$ is the Lagrangian multiplier corresponding to equation (6b). Taking the partial derivatives to $\dot{\boldsymbol{\tau}}$ and $\boldsymbol{\lambda}$, we can naturally conduct the following equations:

$$\frac{\partial L}{\partial \dot{\boldsymbol{\tau}}} = H\dot{\boldsymbol{\tau}} + W^{\mathrm{T}}\boldsymbol{\lambda} = 0, \tag{8a}$$

$$\frac{\partial L}{\partial \boldsymbol{\lambda}} = \boldsymbol{\omega}_{\mathrm{d}} - W\dot{\boldsymbol{\tau}} = 0. \tag{8b}$$

Note that (8) is a nonlinear equation set that is difficult to get the solution directly, so we need to devise a corresponding RNN to find its numerical solution [35], [46]. According to previous researchers' work [6], [47], the RNN can be derived from equation (8) as follows:

$$\delta\ddot{\boldsymbol{\tau}} = -\dot{\boldsymbol{\tau}} + P_{\Omega}(\dot{\boldsymbol{\tau}} - H\dot{\boldsymbol{\tau}} - W^{\mathrm{T}}\boldsymbol{\lambda}), \tag{9a}$$

$$\delta\dot{\boldsymbol{\lambda}} = \boldsymbol{\omega}_{\mathrm{d}} - W\dot{\boldsymbol{\tau}}, \tag{9b}$$

where $0 < \delta < 1$ is a coefficient for controlling the convergence rate of RNN and usually is set to a teeny-tiny value; P_{Ω} is the projection operator defined as $P_{\Omega}(a) = \mathrm{argmin}_{b\in\Omega}||b-a||$, which imposes the physical limits to the robotic system and $||\cdot||$ is the two-norm of a vector.

Remark 2: Through the above derivations, the RNN for the MKE scheme on the dual-arm robotic system is successfully constructed with physical constraints, and the corresponding solution is shown as well. It is worth mentioning that the value of δ influences the convergence rate of the RNN, and further affects the control effect of the robotic system.

III. Simulations

In this section, we use a dual-arm robotic system named Baxter for the simulation, which has two identical redundant manipulators with 7 DOFs, and the corresponding D-H parameters are shown in Table I. In the simulation, two manipulators are given path tracking tasks and move along the predefined trajectories. The left manipulator will follow a circular path, while the right manipulator will track a tricuspid valve path. The duration of the task T is set to 10 seconds,

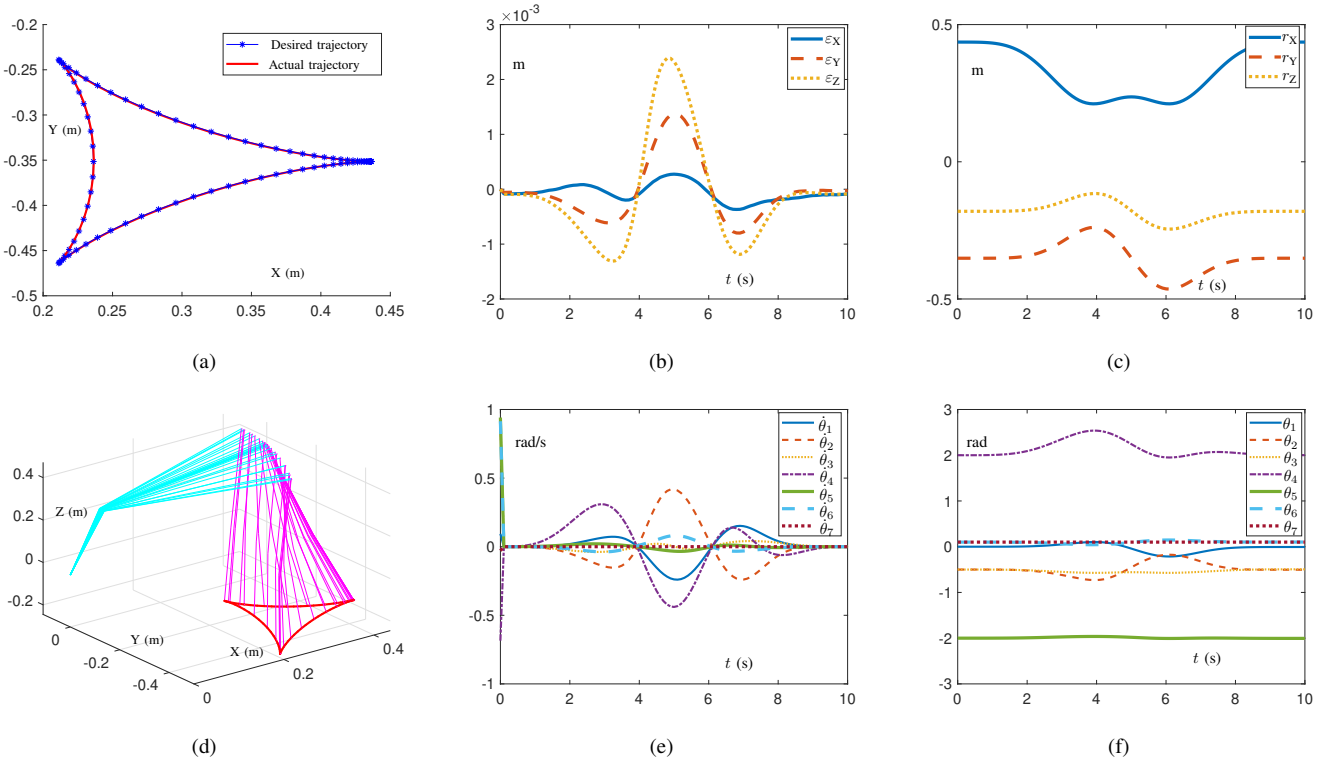

Fig. 2. The simulation results of the right manipulator on the Baxter robot. (a) Real trajectory and desired trajectory of the right manipulator. (b) Time history of the end-effector errors on the right manipulator during the task. (c) Time history of the end-effector positions on the right manipulator during the task. (d) The motion trajectories of the right manipulator. (e) Time history of the joint velocities of the right manipulator. (f) Time history of the joint angles of the right manipulator.

and the convergence rate δ of the RNN is set to 10^{-3} for an excellent simulation result. Besides, the movements of the two manipulators are visualized in the robot visualization system CoppeliaSim.

A. *Left arm path-tracking example*

In the left arm tracking example, the redundant manipulator is given a circle trajectory to track, and the radius of the trajectory is set to 0.08 m; the initial state of the manipulator is set to $[0, -0.5, -0.5, 2, -2, 0.1, 0.1]^{\mathrm{T}}$ rad. The simulation results of the left arm are displayed in Fig. 1. The real trajectory and desired trajectory of the manipulator are depicted in Fig. 1(a), from which we can see the real path and desired path coincide well. Figure 1(b) shows the time history of the end-effector position errors, keeping the order of 10^{-4} m. Figure 1(c) displays the time history of the end-effector positions, and we can find that the fluctuations are very smooth. Figure 1(d) displays the trajectories of manipulator's joints. Figure 1(e) shows the time history of joint velocities, and we can see that the joint velocities are varying within a small range and satisfy the physical constraints of the manipulator. Figure 1(f) shows the time history of joint angles during the task.

B. *Right arm path-tracking example*

In the right arm path tracking example, the redundant manipulator is given a three-valves path tracking task, and the radius of the trajectory is set to 0.05 m; the initial state of the manipulator is the same as the left manipulator. The simulation results are displayed in Fig. 2. The real trajectory and the desired trajectory of the manipulator are shown in Fig. 2(a), from which we can find that the real trajectory is consistent well with the desired trajectory. Figure 2(b) shows the time history of the end-effector position errors, which fluctuate at the order of 10^{-4} m. Figure 2(c) shows the time history of the end-effector positions; Fig. 2(d) displays the trajectories of the manipulator's joints, from which we can see that the joints move smoothly and do not reach the singular states. Figure 2(e) presents the time history of the manipulator's joint velocities, and the joint velocities fluctuate in a small range within the physical constraints. Figure 2(f) depicts the time history of joint positions, and we can see that the joint positions fluctuate very smoothly.

C. *CoppeliaSim simulative results*

Figure 3 depicts snapshots of simulative results in the CoppeliaSim robot visualization system when the Baxter robot is executing the given task. The initial state of the Baxter robot in the visualization system is the same as the state in simulation results, and the data source of the visualization system is generated by simulation in MATLAB. Therefore, this part can be seen as a supplement to simulation results. The six subfigures depict the robot state at different time instants during the task. From Fig. 3, we can see that the left redundant manipulator and the right redundant manipulator of the Baxter

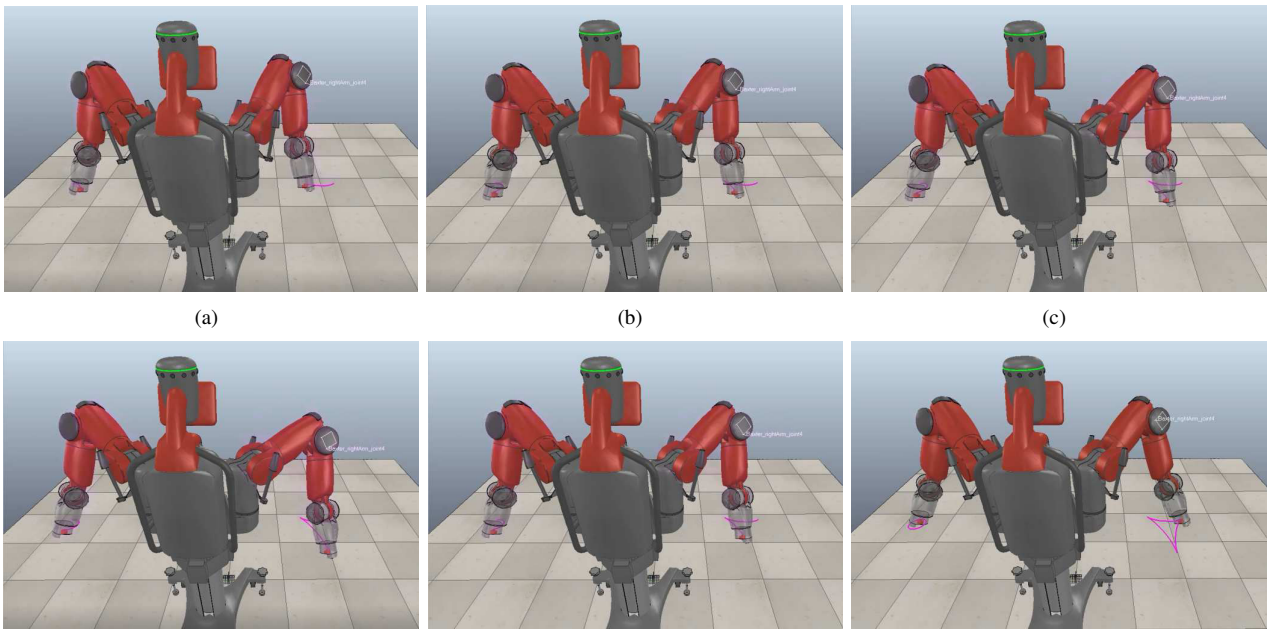

Fig. 3. The snapshots of the simulative results on Baxter robot in CoppeliaSim visualization system for the left arm and right arm executing two trajectories tracking path, respectively.

robot start executing their tasks simultaneously and finish the task at the same time. From figures drawn by the left and right manipulators, we can observe that the task is perfectly executed, which verifies the efficiency and accuracy of the solution for the MKE scheme on the dual-arm robotic system in a further step.

IV. Conclusion

In this paper, the MKE performance index has been investigated on the dual-arm robotic system. First, the schemes of the left manipulator and right manipulator have been investigated, respectively. Then, the two schemes have been unified into one scheme and transformed into a QP problem. For solving the problem, an RNN has been devised aided with the Lagrange multiplier method. Finally, to verify the correctness of the solution for the unified QP problem, computer simulations and simulative experiments on a dual-arm robotic system named Baxter have been carried out. The simulative results demonstrate that the MKE scheme on dual-arm robotic systems has been successfully figured out. It is worth mentioning that the formulated scheme can be extended to multi-arm robotic systems, not just limited to dual-arm robotic systems. Momentously, the MKE scheme is first extended to dual/multi-arm robotic systems in this work, which can be considered as a meaningful innovation in the redundant manipulator field.

References

[1] Y. Zhong, L. Jin, M. Shang, and X. Luo, "Momentum-incorporated symmetric non-negative latent factor models," *IEEE Trans. Big Data*, In Press with DOI: 10.1109/TBDATA.2020.3012656.

[2] X. Luo, H. Wu, H. Yuan, and M. Zhou, "Temporal pattern-aware QoS prediction via biased non-negative latent factorization of tensors," *IEEE Trans. Cybern.*, vol. 50, no. 5, pp. 1798–1809, May 2020.

[3] X. Luo, M. Zhou, Z. Wang, Y. Xia, and Q. Zhu, "An effective scheme for QoS estimation via alternating direction method-based matrix factorization," *IEEE Trans. Services Comput.*, vol. 12, no. 4, pp. 503–518, 1 Jul.-Aug. 2019.

[4] R. Iizuka, S. Miyahara, and D. N. Nenchev, "Walking with hand motion/force control and CoM/VRP and trunk compliance for disturbance accommodation," *IEEE Robot. Autom. Lett.,* vol. 5, no. 1, pp. 203–210, Jan. 2020.

[5] Z. Li, S. S. Ge, and S. Liu, "Contact-force distribution optimization and control for quadruped robots using both gradient and adaptive neural networks," *IEEE Trans. Neural Netw. Learn. Syst.,* vol. 25, no. 8, pp. 1460–1473, Aug. 2014.

[6] L. Jin, S. Li, H. M. La, and X. Luo, "Manipulability optimization of redundant manipulators using dynamic neural networks," *IEEE Trans. Ind. Electron,* vol. 64, no. 6, pp. 4710–4720, Jun. 2017.

[7] J. Zhang, L. Jin, and L. Cheng, "RNN for perturbed manipulability optimization of manipulators based on a distributed scheme: A game-theoretic perspective," *IEEE Trans. Neural Netw. Learn. Syst.,* vol. 31, no. 12, pp. 5116–5126, Dec. 2020.

[8] B. Cai and Y. Zhang, *Optimal and efficient motion planning of redundant robot manipulators.* Germany: LAMBERT Academic Publishing, 2013.

[9] D. Guo, K. Zhai, Z. Xiao, H. Tan, and Y. Zhang, "Acceleration-level minimum kinetic energy (MKE) scheme derived via Ma equivalence for motion planning of redundant robot manipulators," in *proceedings of 2014 Seventh International Symposium on Computational Intelligence and Design,* Hangzhou, China, 2014, pp. 26–30.

[10] D. Guo and Y. Zhang, "Simulation and experimental verification of weighted velocity and acceleration minimization for robotic redundancy resolution," *IEEE Trans. Autom. Sci. Eng.,* vol. 11, no. 4, pp. 1203–1217, Oct. 2014.

[11] X. Luo, Z. Liu, S. Li, M. Shang, and Z. Wang, "A fast non-negative latent factor model based on generalized momentum method," *IEEE Trans. Syst., Man, Cybern. Syst.*, vol. 51, no. 1, pp. 610–620, Jan. 2021.

[12] X. Luo, M. Zhou, S. Li, D. Wu, Z. Liu, and M. Shang, "Algorithms of unconstrained non-negative latent factor analysis for recommender systems," *IEEE Trans. Big Data*, vol. 7, no. 1, pp. 227–240, Mar. 2021.

[13] X. Luo, M. Zhou, S. Li, Y. Xia, Z. You, Q. Zhu, and H. Leung, "Incorporation of efficient second-order solvers into latent factor models for accurate prediction of missing QoS data," *IEEE Trans. Cybern.*, vol. 48, no. 4, pp. 1216–1228, Apr. 2018.

[14] X. Luo, M. Zhou, S. Li, Z. You, Y. Xia, and Q. Zhu, "A nonnegative latent factor model for large-scale sparse matrices in recommender systems via alternating direction method," *IEEE Trans. Neural Netw. Learn. Syst.*, vol. 27, no. 3, pp. 579–592, Mar. 2016.

[15] X. Luo and M. Zhou, "Effects of extended stochastic gradient descent algorithms on improving latent factor-based recommender systems," *IEEE Robot. Autom. Lett.*, vol. 4, no. 2, pp. 618–624, Apr. 2019.

[16] X. Luo, D. Wang, M. Zhou, and H. Yuan, "Latent factor-based recommenders relying on extended stochastic gradient descent algorithms," *IEEE Trans. Syst., Man, Cybern. Syst.*, vol. 51, no. 2, pp. 916–926, Feb. 2021.

[17] X. Luo, W. Qin, A. Dong, K. Sedraoui, and M. Zhou, "Efficient and high-quality recommendations via momentum-incorporated parallel stochastic gradient descent-based learning," *IEEE/CAA J. Automatica Sinica*, vol. 8, no. 2, pp. 402–411, February 2021.

[18] X. Luo, M. Zhou, Y. Xia, and Q. Zhu, "An incremental-and-static-combined scheme for matrix-factorization-based collaborative filtering," *IEEE Trans. Autom. Sci. Eng.*, vol. 13, no. 1, pp. 333–343, Jan. 2016.

[19] X. Luo, M. Zhou, S. Li, L. Hu, and M. Shang, "Non-negativity constrained missing data estimation for high-dimensional and sparse matrices from industrial applications," *IEEE Trans. Cybern.*, vol. 50, no. 5, pp. 1844–1855, May 2020.

[20] J. Chen and X. Luo, "Randomized latent factor model for high-dimensional and sparse matrices from industrial applications," in *proceedings of 2018 IEEE 15th International Conference on Networking, Sensing and Control (ICNSC),* pp. 1–7, 2018.

[21] X. Luo, M. Zhou, S. Li, and M. Shang, "An inherently nonnegative latent factor model for high-dimensional and sparse matrices from industrial applications," *IEEE Trans. Ind. Informat.*, vol. 14, no. 5, pp. 2011–2022, May 2018.

[22] X. Luo, J. Sun, Z. Wang, S. Li, and M. Shang, "Symmetric and nonnegative latent factor models for undirected, high-dimensional, and sparse networks in industrial applications," *IEEE Trans. Ind. Informat.*, vol. 13, no. 6, pp. 3098–3107, Dec. 2017.

[23] L. Hu, X. Yuan, X. Liu, S. Xiong, and X. Luo, "Efficiently detecting protein complexes from protein interaction networks via alternating direction method of multipliers," *IEEE/ACM Trans. Comput. Biol. Bioinform.*, vol. 16, no. 6, pp. 1922–1935, 1 Nov.-Dec. 2019.

[24] Y. Song, M. Li, X. Luo, G. Yang, and C. Wang, "Improved symmetric and nonnegative matrix factorization models for undirected, sparse and large-scaled networks: A triple factorization-based approach," *IEEE Trans. Ind. Informat.*, vol. 16, no. 5, pp. 3006–3017, May 2020.

[25] L. Hu, P. Hu, X. Luo, X. Yuan, and Z. -H. You, "Incorporating the coevolving information of substrates in predicting HIV-1 protease cleavage sites," *IEEE/ACM Trans. Comput. Biol. Bioinf.*, vol. 17, no. 6, pp. 2017–2028, 1 Nov.-Dec. 2020.

[26] L. Jin, J. Yan, X. Du, X. Xiao, and D. Fu, "RNN for solving time-variant generalized Sylvester equation with applications to robots and acoustic source localization," *IEEE Trans. Ind. Informat.*, vol. 16, no. 10, pp.6359–6369, Oct. 2020.

[27] Y. Liufu, L. Jin, J. Xu, X. Xiao, and D. Fu, "Reformative noise-immune neural network for equality-constrained optimization applied to image target detection,"*IEEE Trans. Emerg. Topics Comput.*, In Press with DOI: 10.1109/TETC.2021.3057395.

[28] J. Zhang, L. Jin, and C. Yang, "Distributed cooperative kinematic control of multiple robotic manipulators with improved communication efficiency," *IEEE/ASME Trans. Mechatronics*, In Press with DOI: 10.1109/TMECH.2021.3059441.

[29] J. Zhang, L. Jin, and L. Cheng, "RNN for perturbed manipulability optimization of manipulators based on a distributed scheme: A game-theoretic perspective," *IEEE Trans. Neural Netw. Learn. Syst.*, vol. 31, no. 12, pp. 5116–5126, Dec. 2020.

[30] Mindspore. https://www.mindspore.cn/, 2020.

[31] Z. Xie, L. Jin, X. Luo, Z. Sun, and M. Liu, "RNN for repetitive motion generation of redundant robot manipulators: An orthogonal projection-based scheme," *IEEE Trans. Neural Netw. Learn. Syst.,* In Press with DOI: 10.1109/TNNLS.2020.3028304.

[32] H. Lu, L. Jin, X. Luo, B. Liao, D. Guo, and L. Xiao, "RNN for solving perturbed time-varying underdetermined linear system with double bound limits on residual errors and state variables," *IEEE Trans. Ind. Informat.,* vol. 15, no. 11, pp. 5931–5942, Nov. 2019.

[33] S. Li, Z. Shao and Y. Guan, "A dynamic neural network approach for efficient control of manipulators," *IEEE Trans. Syst., Man, Cybern. Syst.,* vol. 49, no. 5, pp. 932–941, May 2019.

[34] Z. Xu, S. Li, X. Zhou, S. Zhou, T. Cheng, and Y. Guan, "Dynamic neural networks for motion-force control of redundant manipulators: An optimization perspective," *IEEE Trans. Ind. Electron.,* vol. 68, no. 2, pp. 1525–1536, Feb. 2021.

[35] S. Li, H. Wang, and M. U. Rafique, "A novel recurrent neural network for manipulator control with improved noise tolerance," *IEEE Trans. Neural Netw. Learn. Syst.,* vol. 29, no. 5, pp. 1908–1918, May 2018.

[36] L. Jin and Y. Zhang, "G2-type SRMPC scheme for synchronous manipulation of two redundant robot arms," *IEEE Trans. Cybern.,* vol. 45, no. 2, pp. 153–164, Feb. 2015.

[37] C. Alford and S. Belyeu, "Coordinated control of two robot arms," in *proceedings of 1984 IEEE International Conference on Robotics and Automation,* Atlanta, GA, USA, 1984, pp. 468–473.

[38] Y. Zhang, M. Yang, D. Chen, W. Li, D. Guo, and X. Yan, "Proposing, QP-unification and verification of DLSM based MKE-IIWT scheme for redundant robot manipulators," in *proceedings of 2017 IEEE 3rd Information Technology and Mechatronics Engineering Conference (ITOEC),* Chongqing, China, 2017, pp. 242–248.

[39] D. Guo, X. Yan, L. Jin, H. Tan, and Y. Zhang, "ZE in iZ1eD1 manner for MKE redundancy resolution at velocity and acceleration levels," in *proceedings of 2014 2nd International Conference on Systems and Informatics (ICSAI 2014),* Shanghai, China, 2014, pp. 45–50.

[40] Y. Zhang, S. S. Ge, and T. H. Lee, "A unified quadratic-programming-based dynamical system approach to joint torque optimization of physically constrained redundant manipulators," *IEEE Trans. Syst. Man Cybern. B Cybern.,* vol. 34, no. 5, pp. 2126–2132, Oct. 2004.

[41] Y. Zhang, J. Wang, and Y. Xia, "A dual neural network for redundancy resolution of kinematically redundant manipulators subject to joint limits and joint velocity limits," *IEEE Trans. Neural Netw.,* vol. 14, no. 3, pp. 658–667, May 2003.

[42] Z. Xie, L. Jin, X. Du, X. Xiao, H. Li and S. Li, "On generalized RMP scheme for redundant robot manipulators aided with dynamic neural networks and nonconvex bound constraints," in *IEEE Transactions on Industrial Informatics,* vol. 15, no. 9, pp. 5172-5181, Sep. 2019.

[43] A. Smith, C. Yang, C. Li, H. Ma, and L. Zhao, "Development of a dynamics model for the Baxter robot," in *proceedings of 2016 IEEE International Conference on Mechatronics and Automation,* Harbin, China, 2016, pp. 1244–1249.

[44] Y. Xia, G. Feng, and J. Wang, "A novel recurrent neural network for solving nonlinear optimization problems with inequality constraints," in *IEEE Trans. Neural Netw.,* vol. 19, no. 8, pp. 1340–1353, Aug. 2008.

[45] L. Jin, Z. Xie, M. Liu, K. Chen, C. Li, and C. Yang, "Novel joint-drift-free scheme at acceleration level for robotic redundancy resolution with tracking error theoretically eliminated," *IEEE/ASME Trans. Mechatronics*, vol. 26, no. 1, pp. 90–101, Feb. 2021.

[46] Z. Xie, L. Jin, X. Luo, S. Li, and X. Xiao, "A data-driven cyclic-motion generation scheme for kinematic control of redundant manipulators," *IEEE Trans. Control Syst. Technol.*, vol. 29, no. 1, pp. 53–63, Jan. 2021.

[47] L. Jin, S. Li, and B. Hu, "RNN models for dynamic matrix inversion: A control-theoretical perspective," *IEEE Trans. Ind. Informat.,* vol. 14, no. 1, pp. 189–199, Jan. 2018.